

The Star Formation Rate in disk galaxies: thresholds and dependence on gas amount

S. Boissier¹*, N. Prantzos², A. Boselli³ and G. Gavazzi⁴

¹*Carnegie Observatories, 813 Santa Barbara Street, Pasadena, California 91101, USA*

²*Institut d’Astrophysique de Paris, 98bis Bd. Arago, 75104 Paris, France*

³*Laboratoire d’Astrophysique de Marseille, Traverse du Siphon, F-13376 Marseille Cedex 12, France*

⁴*Università degli Studi di Milano - Bicocca, Piazza dell’Ateneo Nuovo 1, 20126 Milano, Italy*

submitted july 2003

ABSTRACT

We reassess the applicability of the Toomre criterion in galactic disks and we study the local star formation law in 16 disk galaxies for which abundance gradients are published. The data we use consists of stellar light profiles, atomic and molecular gas (deduced from CO with a metallicity-dependent conversion factor), star formation rates (from H_α emissivities), metallicities, dispersion velocities and rotation curves. We show that the Toomre criterion applies successfully to the case of the Milky Way disk, but it has limited success with the data of our sample; depending on whether the stellar component is included or not in the stability analysis, we find average values for the threshold ratio of the gas surface density to the critical surface density in the range 0.5 to 0.7. We also test various star formation laws proposed in the literature, i.e. either the simple Schmidt law or modifications of it, that take into account dynamical factors. We find only small differences among them as far as the overall fit to our data is concerned; in particular, we find that all three SF laws (with parameters derived from the fits to our data) match particularly well observations in the Milky Way disk. In all cases we find that the exponent n of our best fit SFR has slightly higher values than in other recent works and we suggest several reasons that may cause that discrepancy.

Key words: Galaxies: general, spiral, evolution

1 INTRODUCTION

Star formation is the main driver of galactic evolution. Despite four decades of intense observational and theoretical investigation (see e.g. Elmegreen 2002 for a recent overview) our understanding of the subject remains frustratingly poor. As a result, important questions related e.g. to the putative threshold and to the rate of star formation in galaxies have no clear answers yet.

In most (if not all) studies of galaxy evolution, empirical formulae are used to describe the star formation. Such formulae are based on the original suggestion by Schmidt (1959), namely that the star formation rate (SFR) is simply proportional to some power n of the gas mass density ρ . In the case of disk galaxies and starbursts observations (Kennicutt 1998b) suggest that such a relation indeed holds when gas surface density Σ_{GAS} is used instead of the mass density and when quantities are averaged over the whole optical disk; in that case, the exponent n is found to be close

to 1.5. However, Kennicutt (1998b) noted that other interpretations of the data are possible: in particular, an equally good fit to the data is obtained when it is assumed that gas turns into stars within a dynamical timescale (taken to be the orbital timescale at the optical radius).

Such “global” laws may be useful for some applications (like e.g. semi-analytical models of galaxy evolution) but for detailed models of galactic disks “local” SF laws are required. Several such laws have been suggested either on observational (e.g. Dopita & Ryder, 1994) or theoretical grounds (e.g. dynamical instabilities in spirals, Ohnishi 1975, Wyse & Silk 1989). In a recent work, Wong & Blitz (2002) find that the simple Schmidt law is valid locally, with $n=1.1$ –1.7 (depending on whether extinction on the observed H_α emissivity profiles of their disks is assumed to be uniform or dependent on gas column density). They also find that a dynamically modified Schmidt law (i.e. by introducing the orbital timescale as Kennicutt 1998b) gives also an acceptable fit to their data.

The question of a threshold in star formation in galactic disks has been observationally assessed by Kennicutt (1989),

* E-mail:boissier@ociw.edu

who found that star formation is strongly suppressed below $\Sigma_{GAS} \sim 5-10 M_{\odot} \text{ pc}^{-2}$. The existence of such a threshold is indeed suggested by dynamical stability analysis of thin, gaseous, differentially rotating disks (e.g. Toomre 1964, Quirk 1972). In a recent investigation, Martin and Kennicutt (2001) found that the threshold gas density (measured at the edge of the star forming disk) varies by at least an order of magnitude among spiral galaxies, but the ratio of gas density to a critical density (see Sect. 4 for its definition) is much more uniform. Martin & Kennicutt (2001) also identified the limitations of their observational strategy: uncertainties associated with non axisymmetric gas distributions and with the extrapolation of the molecular gas density profile, from the last observed point to the edge of the star forming disk. The latter issue was properly studied by Wong & Blitz (2002) with the help of detailed molecular profiles, but for a limited sample of spirals, particularly rich in molecular gas. Their conclusion is that the gravitational stability criterion has only a limited application.

From the theoretical point of view, quite a lot of work has been done to include more physics in the analysis than the simple stability criterion (e.g. Toomre 1981, Elmegreen 1987, Romeo 1992, Wang & Silk 1994 etc.) The general conclusion is that the various physical factors (stars, magnetic fields, turbulence) affect only slightly the stability parameter, by a factor of order unity.

In a recent work Schaye (2002) reassesses the role of the gas velocity dispersion in the application of the simple stability criterion. He suggests that the usual assumption of a constant dispersion over the disk may not hold and he investigates the stability of thin, gaseous, self-gravitating disks imbedded in dark halos and illuminated by UV radiation. He finds that the drop in the velocity dispersion associated with the transition from a warm to a cold phase of the interstellar medium (i.e. from $\sim 10^4$ K to below 10^3 K) causes the disk to become gravitationally unstable. This analysis leads to prescriptions for evaluating threshold surface densities as a function of metallicity, intensity of UV radiation, and gaseous fraction. However, a major prediction of his model analysis seems to be contradicted by observations. Indeed, he finds that at the phase transition there is always a sharp increase in the molecular gas fraction, whereas Martin & Kennicutt (2001) find that at the thresholds of their star forming disks the gas is primarily atomic (for the low gas surface densities) or molecular (for the highest gas surface densities), i.e. no clear sign of a phase transition.

In this work, we reassess the applicability of the Toomre criterion in galactic disks and we study the local star formation law by means of a homogeneous sample containing 16 spirals, half of which belong to the Virgo cluster. In Sect. 2 we present our data sample, which consists of profiles of stars, atomic and molecular gas, star formation rates (from H_{α} emissivities), metallicities and rotation curves. In Sect. 3 we present briefly the theoretical background of the stability criterion, including a modification suggested by Wang & Silk (1994). We show that it applies successfully to the case of the Milky Way disk (Sect. 3.2) but it has limited success with the data of our sample. In Sect. 4 we test various SF laws proposed in the literature, i.e. either the simple Schmidt law or modifications of it, that take into account dynamical factors. We find only small differences among them as far as the overall fit to our data is concerned; in particular, we

find that all three SF laws (with parameters derived from the fits to our data) match particularly well observations in the Milky Way disk. In all cases we find that the exponent n of our best fit SFR has slightly higher values than in other recent works and we suggest several reasons that may cause that discrepancy. Our results are summarised in Sect. 5.

2 OBSERVATIONAL DATA

2.1 The galaxy sample

The galaxies of our sample were selected for a detailed study of the star formation properties in nearby spirals. Our first requirement was that abundance measurements in HII regions are available so that a metallicity gradient is defined. The molecular gas profile can then be deduced from CO observations with a metallicity dependent conversion factor recently determined (see Boselli et al., 2002 and Sec. 2.3 below). For this reason, these galaxies do not form a complete sample in any sense but are the ones for which the metallicity-dependent conversion factor can be used. An accurate estimate of the radial profile of atomic gas and of the star formation rate (here deduced from H_{α} emission line intensities) is also required for our purpose. Some of the proposed instability criteria in galactic disks involve the rotation frequency (requiring knowledge of the rotation curve), the stellar surface density profile (obtained from the H and K band profiles), and also the velocity dispersion of the stellar component (derived in Sec. 3.1).

The final list of galaxies, only selected to have abundance gradients published and the other data needed for our analysis, includes 16 galaxies, 7 of them “isolated” and 9 belonging to the Virgo cluster (most of the data concerning the Virgo galaxies are available via the goldmine database, Gavazzi et. al, 2003). Note that some of the “isolated” galaxies are in fact part of small groups (NGC2403, 3031, 4258, 5194).

In order to estimate the degree of perturbation induced by the interaction of a galaxy with its environment, we use the *HI deficiency parameter*, defined as $\text{HI def.} = \log(\langle \text{HI} \rangle / \text{HI})$, the ratio of the average HI mass in isolated objects of similar morphological type and linear size to the HI amount of an individual galaxy (Haynes & Giovanelli (1984)). The sample includes both gas deficient ($\text{HI def.} > 0.3$) and gas rich galaxies to study whether their SFR profiles are affected by the amount of available gas. It has been selected to span the largest possible range in gas column density within late-type galaxies of similar type.

Information on the galaxies of the adopted sample is given in Table 1. Column 1 gives the name of the galaxy and Column 2 the blue magnitude. Column 3 gives the galaxy distance. A distance of 17 Mpc is adopted for all the Virgo galaxies. We adopt the distance deduced from the brightest stars of NGC2903 (Drozdovsky & Karachentsev 2000) and the planetary nebulae distance of NGC5194 by Feldmeier et al. (1997). For the other galaxies of the sample, Cepheid distances were deduced in the framework of the HST key project (Freedman et al. 2001). Column 4 gives the morphological type. Column 5 gives the logarithm of the HI velocity width W_C (in km s^{-1}), corrected for inclination as in Gavazzi (1987). Column 6 gives the HI-deficiency, computed as in Haynes & Giovanelli (1984), from the integrated

Table 1. The sample of galaxies used in this study. Properties are given in Cols 2-6 and References for the data in Cols 7-11. Description of the Table entries is made in Sect. 2. The first half of the Table concerns nearby galaxies, while the second half refers to Virgo galaxies.

Galaxy (1)	m_B (mag) (2)	Dist.(Mpc) (3)	Type (4)	$\log(W_C)$ (5)	HI def. (6)	HI (7)	CO (8)	Z (9)	H_{α} (10)	V(R) (11)	Photometry (12)
NGC925	10.69	9.16	SAB(s)d	2.42	0.0	a	f	i,j	o	p	B,V,H
NGC2403	8.93	3.22	SAB(s)cd	2.47	0.1	a	h	i,j,k	o	q,r	B,V,H,K
NGC2541	12.26	11.22	SA(s)cd	2.33	0.7	b	g	j	o	s	U,B,V,H
NGC2903	9.68	8.90	SB(s)d	2.65	0.4	a	h	i,j	o	q,r	U,B,V,H
NGC3031	7.89	3.63	SA(s)ab	2.67	0.1	c	f	j	o	r,t	B,V,H
NGC4258	9.10	7.98	SAB(s)bc	2.68	0.5	a	h	j	o	r,u	B,V,H
NGC5194	8.96	8.40	SA(s)bc-pe	2.76	0.6	d	h	j	o	r	B,V, H
NGC4254	10.44	17.00	SA(s)c	2.76	0.0	e	h	l	o	v,w,x	B,V,H
NGC4303	10.18	17.00	SAB(rs)bc	2.47	-0.1	e	h	l	n	r,x,y,z	B,V,H
NGC4321	10.05	17.00	SAB(s)bc	2.73	0.5	e	h	l	o	r,x,y	U,B,V,H
NGC4501	10.36	17.00	SA(rs)b	2.79	0.5	e	h	l	o	x,y,z	U,B,V,H
NGC4571	11.82	17.00	SA(r)d	2.66	0.5	e	h	l	m	y	B,H
NGC4651	11.39	17.00	SA(rs)c	2.72	-0.2	e	h	l	m	y,z	H
NGC4654	11.10	17.00	SAB(rs)cd	2.56	-0.3	e	h	l	n	v,x,y	B,V,H,K
NGC4689	11.60	17.00	SA(rs)bc	2.47	0.9	e	h	l	n	v,x,y	B,V,K
NGC4713	12.19	17.00	SAB(rs)d	2.35	-0.4	e	—	l	m	v,y	V,H

References: Wevers et al. (1986) [a], Broeils & van Woerden (1994) [b], Rots (1975) [c], Rand et al. (1992) [d], Warmels (1986) [e], Sage (1993) [f], Braine et al. (1993) [g], Young et al. (1995) [h], van Zee et al. (1998) [i], Zaritsky et al. (1994) [j], Garnett et al. (1997) [k], Skillman et al. (1996) [l], Martin & Kennicutt (2001) [m], Hippelein et al., in preparation [n], Boselli & Gavazzi (2002) [o], Pisano, Wilcots, & Elmegreen (1998) [p], Begeman (1987) [q], Sofue et al. (1999) [r], Vega Beltrán et al. (2001) [s], Adler & Westpfahl (1996)[t], van der Kruit (1974) [u], Sperandio et al. (1995) [v], Chincarini & de Souza (1985) [w], Guhathakurta et al. (1988) [x], Rubin, Waterman, & Kenney (1999) [y], Distefano et al. (1990) [z]. The images from which the photometric data are derived are presented for the Virgo galaxies in Boselli et al. (1997, 2000) (H), and Boselli et al. (2003) (optical). For the other galaxies in the infrared: Pierini et al. (1997), Boselli et al. (2000), Zibetti et al., in preparation. The optical data will be presented in a following paper making a larger use of them (Boissier et al., in preparation).

HI masses (Huchtmeier & Richter 1989) and the blue major axes as given in the Uppsala General Catalogue (Nilson 1973).

For each of our galaxies, Table 1 provides also references for the adopted profiles of neutral gas, CO emissivity and oxygen abundance data (columns 7, 8, and 9, respectively). Column 10 presents the sources of the H_{α} data. For the majority of the sample we adopt the results of Boselli & Gavazzi (2002); for three galaxies (m) we use the data kindly made available by Martin & Kennicutt (2001) and for three others (n) data obtained by Hippelein et al. (in preparation).

Column 11 gives references for rotation curves. Finally, Column 12 gives the photometric bands for which we have images, allowing to derive corresponding stellar surface density profiles.

For NGC3031 and NGC4258, we used the H band profile provided in the 2mass large galaxies atlas: <http://www.ipac.caltech.edu/2mass/gallery/largegal/> (Jarrett et al. 2002).

2.2 Atomic gas profiles

With the exception of NGC5194 (HI-map obtained with the VLA), the data were obtained with the Westerbork Radio Telescope (see caption of Table 1). The HI profile given by Broeils & van Woerden (1994) was obtained along the major axis of the galaxy. The data by Wevers et al. (1986), Rots (1975) and Rand et al. (1992) were obtained by integrating HI maps over concentric ellipses.

The data concerning the Virgo galaxies are taken from the thesis of Warmels (Warmels 1986). His data are two dimensional maps for NGC4321, NGC4501, and NGC4651. For the other galaxies, the data were obtained along one (and sometimes two) resolution axis. The maps were inte-

grated onto one resolution axis, and the same procedure was applied to the whole sample to obtain the HI density profiles from the data along one axis.

In all the cases, the HI profiles correspond to a “face-on” orientation. A typical uncertainty of 20 % should be quoted for all the HI profiles, which is smaller than the uncertainties of H_2 profiles (see next section).

2.3 Molecular gas profiles

The adopted CO intensity profiles have been corrected for inclination. The spatial resolution of the CO observations is relatively poor (45") and the measurements were made only along the major axis of each galaxy. On the other hand, the relatively large beams average the CO emission on larger scales and are less affected by small-scale clumpiness.

In their recent study concerning the star formation rate in galactic disks, Wong & Blitz (2002) used high resolution profiles obtained with the BIMA interferometer (Regan et al. 2001) for 7 disk galaxies. The observations of Regan et al. (2001) concern 15 galaxies from which four are in common with our sample (NGC 2903, 4258, 5194, 4321). Their profiles (Figure 3 in Regan et al. 2001) differ from ours in the innermost parts of the galaxies, but we are only interested in galactic discs and not in bulges in this work, so that this difference is not of importance for our conclusions.

The low resolution CO profiles adopted in this work are obviously missing any small scale structure seen in the high resolution profiles of Regan et al. (2001). Our profiles, however, agree well with the low-resolution one also shown in Regan et al. (2001; Fig. 3), which represent a good estimate of the average CO profile in most cases. Among the four galaxies that are common in the two samples, only NGC4258 presents really important variations (\sim one magnitude) on small scales.

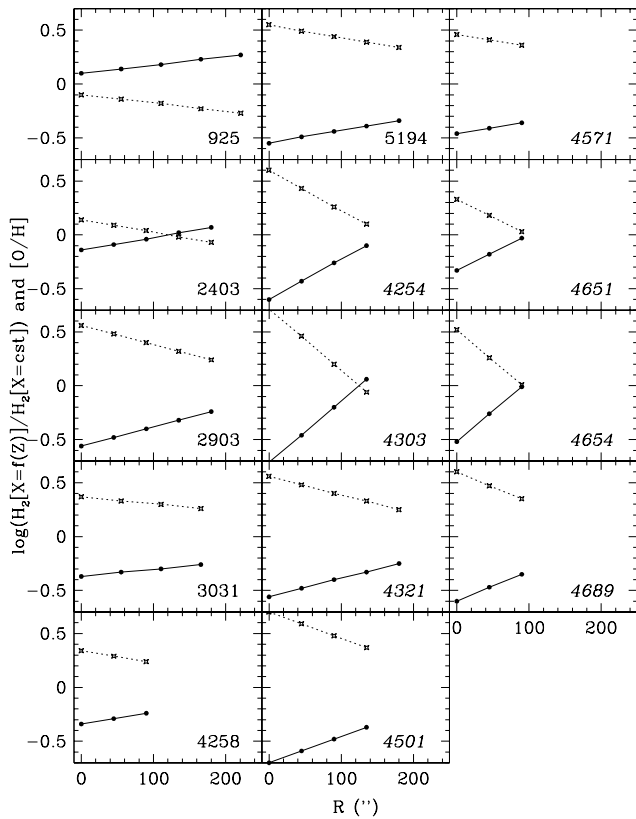


Figure 1. *Solid curves:* Amount of molecular gas obtained by our method (i.e. with metallicity dependent conversion factor of CO to H₂), divided by the amount of molecular gas obtained with a constant conversion factor. Results are plotted as a function of galactocentric radius. *Dotted curves:* The corresponding metallicity profiles [O/H]=log(O/H)-log(O/H)₀. As in the following figures, the name of the Virgo galaxies is indicated in an italic font.

The uncertainty on the H₂ content is much larger than the one of the CO data; it is also more difficult to quantify, since it depends on the poorly known factor X converting CO to H₂. In a recent work Boselli et al. (2002), based on spectro-photometric data available for a small number of nearby galaxies and on a larger sample of late type galaxies with multi-frequency data, found that X depends on metallicity (or luminosity) and they parameterised that dependence as:

$$\log X = -1.01 (12. + \log(O/H)) + 29.28 \quad (1)$$

i.e. the conversion factor is essentially inversely proportional to metallicity. While this correlation was found for integrated values over whole galaxies, we make the assumption that it is also valid for radial profiles. This assumption agrees with the analysis of M51 done by Nakai & Kuno (1995) that, based on the measured radial variation of the dust to gas ratio, brought to similar results.

We transformed CO data into molecular H₂ surface density using the metallicity dependent conversion factor of Equ. 1. We note that the resulting H₂ profile is much poorer in molecular gas, especially in inner galactic regions,

Table 2. Parameters adopted for the determination of the H_α and photometric profiles

Galaxy	Inclination(^o)	PA(^o)
NGC925	54.00	102
NGC2403	60.00	125
NGC2541	66.80	-29
NGC2903	60.00	29
NGC3031	68.00	332
NGC4258	63.00	330
NGC5194	20.00	163
NGC4254	24.51	56
NGC4303	35.99	7
NGC4321	27.37	153
NGC4501	58.62	140
NGC4571	21.09	55
NGC4651	45.24	71
NGC4654	59.05	128
NGC4689	41.01	55
NGC4713	47.80	100

than profiles obtained with a constant factor. In Fig. 1 we show the ratio of the two profiles i.e. the one obtained with a metallicity dependent X divided by the one obtained with a constant X. It is clearly seen that differences by a factor of 2-3 in the inner galaxy are usually obtained.

We note that Wong & Blitz (2002) use a constant conversion factor X, as in fact most studies of SFR in the literature. This explains part of the differences between our study and others (see discussion in Sec. 4.2).

2.4 Star Formation Rate profiles

The star formation rate (SFR) profiles were obtained by subtracting the radial profiles of the continuum near H_α from the H_α+[NII] radial profiles. For three of our galaxies, we used H_α profiles of Martin & Kennicutt (2001), kindly provided by the authors.

The H_α flux was integrated along elliptical annuli with the same PA and inclination as for the HI (see Table 2 for the adopted values). It was corrected for inclination, and translated to a star formation rate as in Boselli et al. (2001). H_α+[NII] fluxes were corrected for [NII] contamination and internal extinction (see Boselli et al. 2001). The conversion from *extinction corrected* H_α flux to star formation rate is obtained assuming a power law IMF of slope -2.5 between 0.1 and 80 M_⊙:

$$SFR(M_{\odot}/\text{yr}) = 0.86 \cdot 10^{-41} L_{H\alpha}(\text{erg/s})$$

As estimated in Boselli et al. (2001), the uncertainties in the IMF, extinction and [NII] contamination correction result in an overall uncertainty of the absolute SFR of a factor ∼ 3.

We note that Wong & Blitz (2002) applied radially dependent extinction corrections to H_α, using the observed gas profiles, an assumed dust to gas ratio, and a given geometry between HI, H₂ and the stars. We prefer here to apply a simple correction for the whole galaxy since, as stressed in Martin & Kennicutt (2001), “radial gradients in internal extinction are typically not strong compared to the scatter in extinction at a given radius”. Moreover, the approach of Wong & Blitz (2002) does not take into account the existence of an abundance gradient within the discs, which is

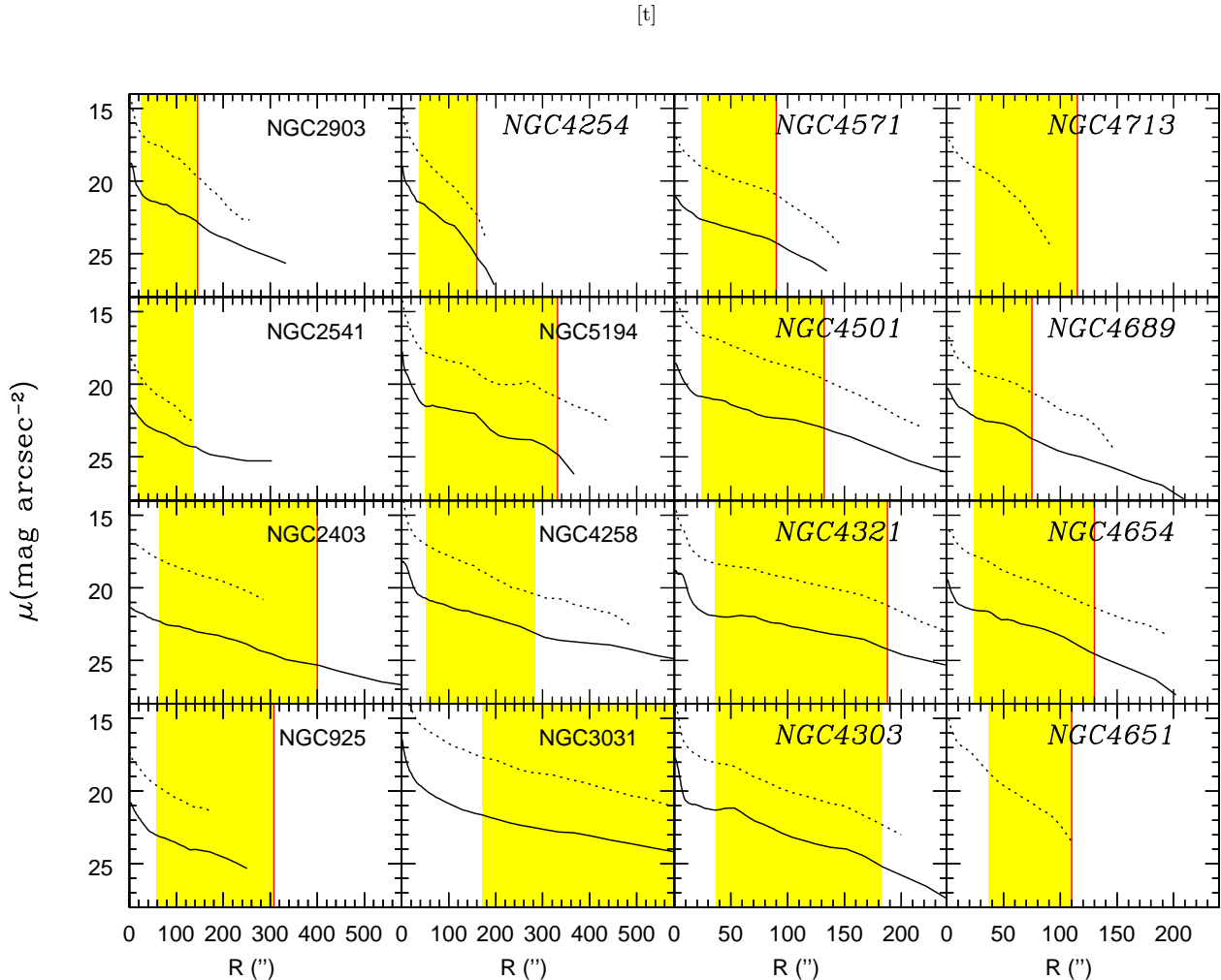


Figure 2. Surface brightness radial profiles in the B-band (solid curves) and in the H-band (dotted curves) for the galaxies of our sample. The grey area is the “disk” region, used for the study of the SFR properties. Its outer radius is either the Martin & Kennicutt (2001) “cut-off” (vertical line, as in Fig. 5) or our own “cut-off” (Sec. 2.8). Its inner radius is the point where the bulge starts dominating over the disk (Sec. 2.6).

likely to affect the dust to gas ratio in different ways at different radii.

2.5 Metallicity profiles

In order to compute the conversion factor X from CO to H_2 , we need the metallicity as a function of radius. Zaritsky et al. (1994), van Zee et al. (1998), Garnett et al. (1997) and Skillman et al. (1996) measured with the same method the oxygen abundances in HII regions located at various galactocentric radii in the sample of our galaxies. From their data, they derived an abundance gradient (slope and intersect at the centre of the galaxy) that we use to estimate the metallicity at each radius (see Fig. 1).

2.6 Photometry

The photometric profiles obtained in the framework of our project were treated in a similar way as the H_α profiles (i.e. they were integrated over ellipses with the same position

angle and inclination, given in table 2). In Fig. 2, we present the B and H-band profiles, which are the most useful for the present work.

We derive a scalelength h_B by an exponential fit to the disc part of the B-band profiles (to be used in section 3.1). The H-band profiles, unaffected by dust extinction, have been used in order to estimate the stellar mass density, assuming the same mass to light ratio as in Boissier et al. (2001). In the case of NGC 4689 the stellar profile was scaled from the K band profile (since the H-band profile was not available), taking into account the total magnitudes in H and K bands, respectively $H=8.32$ and $K=7.76$ (Boselli et al., 1997).

An inspection of the profiles (Fig. 2) shows that in the inner 1 or 2 kpc they present departures from the exponential disc profile, obviously due to the presence of a bulge. These inner regions are ignored in our analysis.

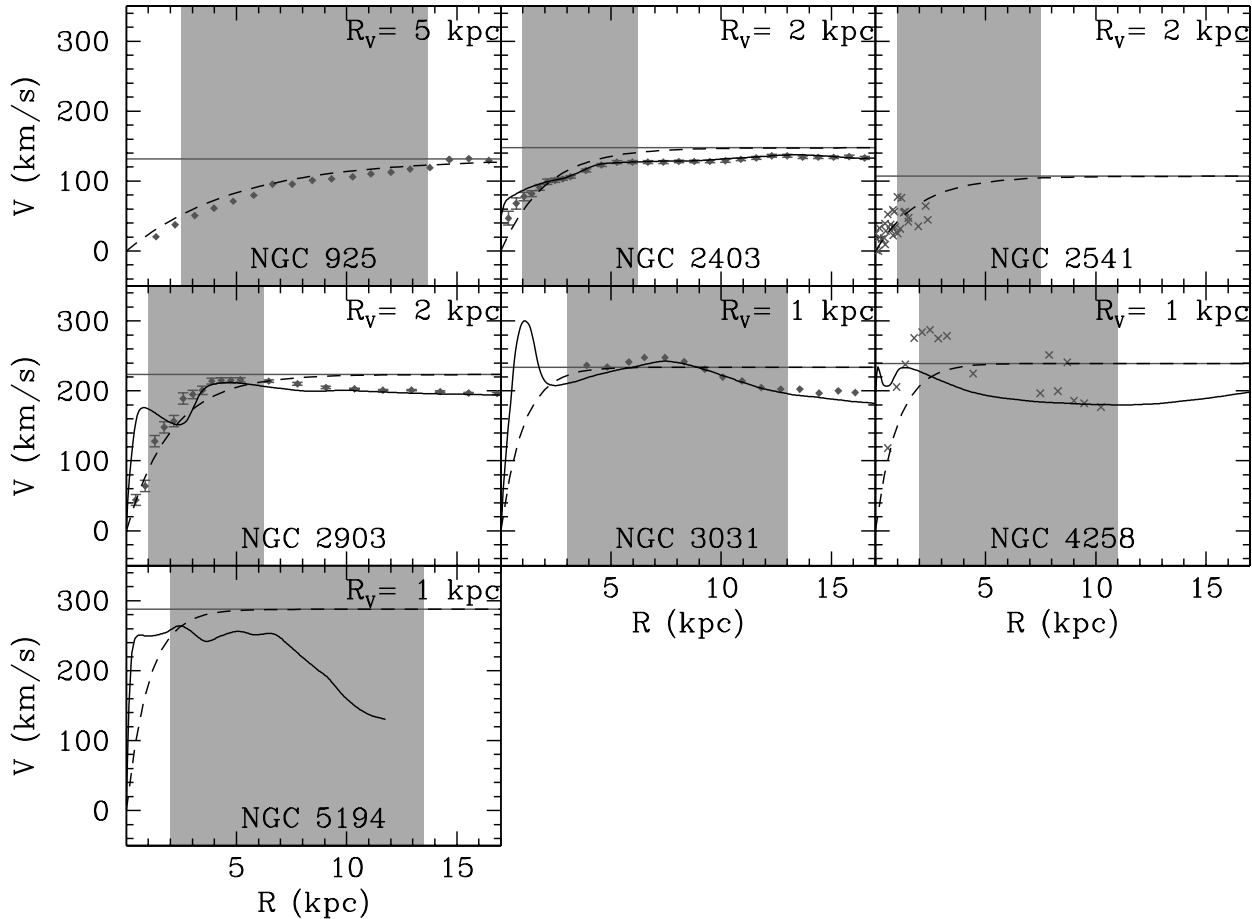


Figure 3. Rotation curves for the isolated galaxies of our sample. *Diamonds*: HI data (Pisano, Wilcots, & Elmegreen (1998) for NGC925, Begeman (1987) for NGC2403 and NGC2903, Adler & Westpfahl (1996) for NGC3031). *Crosses* : Optical slit spectra (van der Kruit (1974) for NGC4258, Vega Beltrán et al. (2001) for NGC2541. The *solid curve* indicates the composite rotation curve of Sofue et al. (1999). The *horizontal line* indicates half the value of the HI line width. The *dashed curve* is the function of Equ. 2, with the corresponding value of R_V indicated for each galaxy. *Shaded areas* indicate the disk region, used for the study of the star formation.

2.7 Rotation curves

The rotation curves of the galaxies of our sample are obtained through a variety of sources: HI rotation curves of Pisano, Wilcots, & Elmegreen (1998), Begeman (1987), Adler & Westpfahl (1996), Guhathakurta et al. (1988), rotation curves derived from optical spectroscopy by van der Kruit (1974), Vega Beltrán et al. (2001), Chincarini & de Souza (1985), Distefano et al. (1990) and for the Virgo galaxies by Rubin, Waterman, & Kenney (1999) and Sperandio et al. (1995). For seven of our galaxies, high resolution curves are given by Sofue et al. (1999), resulting from a combination of CO, optical and HI data.

The adopted rotation curves are presented in figures 3 and 4 for isolated and Virgo galaxies, respectively. In those figures we also indicate by a horizontal line half the value of W_C (the HI line width), in order to show the difference with a flat rotation curve. This constant value usually represents well the “plateau” of the rotation curves, which is not reached at the same radius for all the galaxies. It should

be noted that the data originate from different sources (i.e. studies with different angular resolutions) and present a substantial amount of scatter. For the purpose of homogeneity we approximated the rotation curves with the simple function:

$$V(R) = 0.5 W_C (1 - \exp^{-R/R_V}) \quad (2)$$

At large radii, this approximation produces a plateau at the value W_C given by the HI line width. At small radii, the parameter R_V controls the rise of curve. R_V was adjusted for each galaxy, allowing the curve of equation 2 to reproduce satisfactorily the observed one. This simple representation has the advantages that i) it provides a uniform description of the rotation curve for all galaxies, ii) it has only one free parameter and iii) it can be derived analytically, a useful property for the study of stability criteria in disks (see section 3).

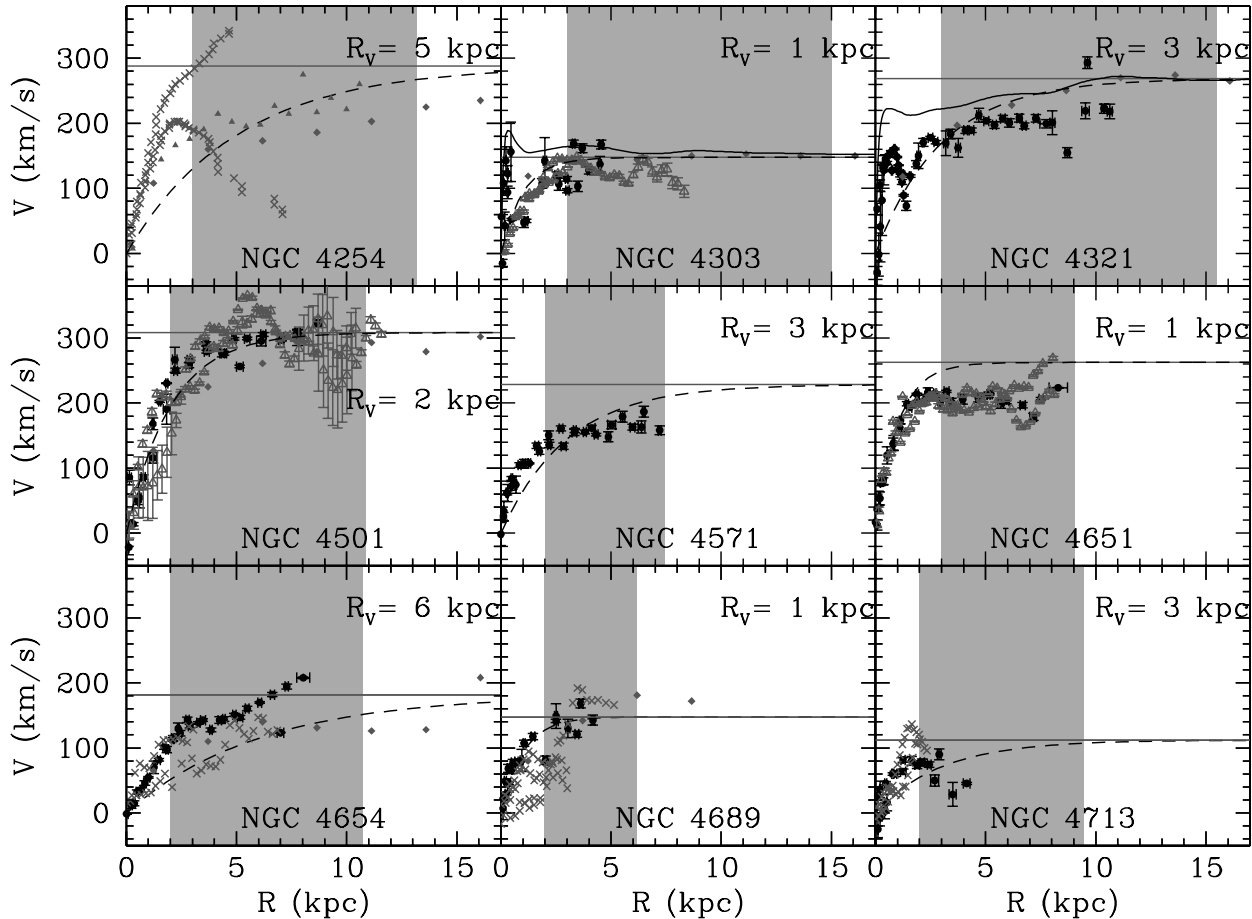


Figure 4. Rotation curves for the Virgo galaxies of our sample. Diamonds: HI data (Guhathakurta et al. 1988). Data of optical slit spectra are from Rubin, Waterman, & Kenney (1999) (filled circles) and Sperandio et al. (1995) (open circles). The solid curve indicates the composite rotation curve of Sofue et al. (1999). As in Fig. 3, the horizontal line indicates half the value of the HI line width, the dashed curve is the function of Equ. 2, with the corresponding value of R_V indicated for each galaxy, shaded areas indicate the disk region, used for the study of the star formation.

2.8 Comments

Our H_2 , HI and SFR surface density profiles are displayed in Fig. 5. Several points should be noted concerning these profiles:

- Resolution is quite different in the profiles of the three major quantities studied. It is low in the case of H_2 , where only 3-5 points are available along the disk; it is satisfactory in the case of HI, with more than 20 points per galaxy, on average; and it is excellent in the case of the H_α profile, where a large number of features appear on the corresponding curves, resulting from azimuthally averaging across the spiral arms. Even if we made an enormous effort of homogenisation, the data are not as deep at all wavelength, in particular for H_2 .

- In most cases, the molecular gas dominates the inner disk, with the exception of NGC2403, NGC4654 and NGC925 (three HI-deficient disks). However, its surface density rarely exceeds $10 M_\odot/pc^2$. Only in one case (NGC5194) does it become as large as $40 M_\odot/pc^2$.

- In general, the HI disk is more extended than the

SFR profile and the latter is more extended than the H_2 profile. In more than half of the cases the SFR becomes negligible (or declines strongly) at the outer limit of the molecular disk. The accurate determination of the molecular gas profile, however, is strongly limited by the difficulty of detecting CO in the low-metallicity, cold outer disc. We shall return to this point concerning a “cut-off” of the SFR in the next section.

3 STABILITY CRITERIA AND SFR THRESHOLD

3.1 Theoretical background

The data presented in Figs. 2, 3, 4 and 5 allow the question of a threshold of the SFR in disk galaxies to be assessed. Such a threshold has been suggested on both observational and theoretical grounds. On the observational side, support comes from the fact that the gaseous layer (HI) is often observed to extend much beyond the stellar disk. On the

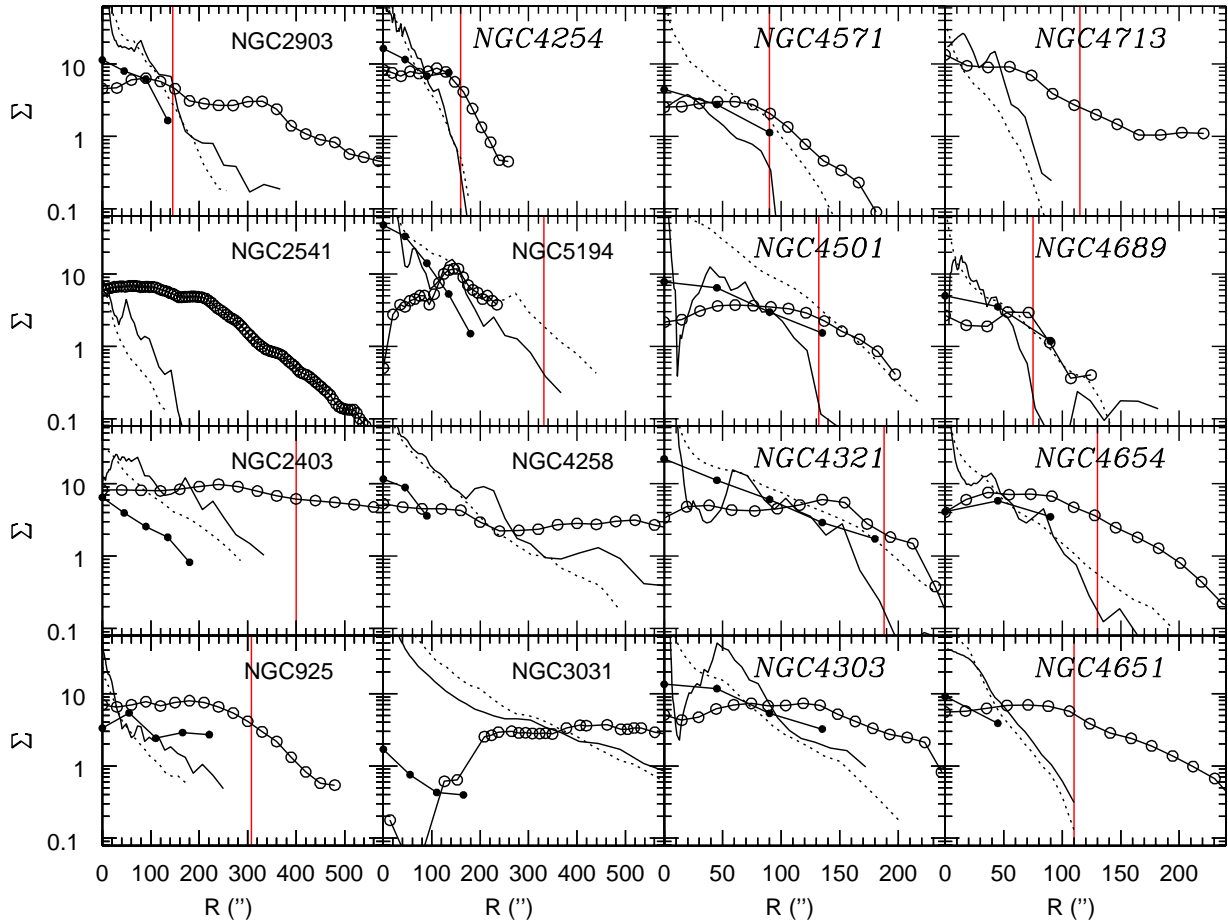


Figure 5. Surface density radial profiles of HI (open circles), H₂ (filled circles), Star Formation Rate (solid curves), and Stellar density (dotted curves). The surface densities of HI and H₂ are in $M_{\odot} \text{ pc}^{-2}$, of stars in $10 M_{\odot} \text{ pc}^{-2}$ and of the star formation rate in $M_{\odot} \text{ pc}^{-2} \text{ Gyr}^{-1}$. The vertical line in some of the panels indicates the SFR “cut-off” found by Martin & Kennicutt (2001). In most cases that line coincides with (or is very close to) a region of steep decline in our own SFR profile.

other hand, the formulation of local instability criteria for differentially rotating disks (Toomre 1964) leads naturally to the idea that large scale star formation may occur only above a critical gas surface density. According to Quirk (1972) this happens when the Toomre parameter

$$Q = \frac{\Sigma_{CRIT}}{\Sigma_{GAS}} < 1 \quad (3)$$

where Σ_{GAS} is the gas surface density and Σ_{CRIT} is given by

$$\Sigma_{CRIT} = \frac{\kappa \sigma_{GAS}}{\pi G} \quad (4)$$

where σ_{GAS} is the local gas velocity dispersion and κ is the local epicyclic frequency, given by

$$\kappa^2 = \frac{2V_C}{R} \left(\frac{dV_C}{dR} + \frac{V_C}{R} \right) \quad (5)$$

where V_C is the gas circular velocity of the galaxy at radius R . For flat rotation curves one has $\kappa = \sqrt{2} V_C/R = \sqrt{2} \Omega$, where Ω is the rotational frequency of the disk.

The gas velocity dispersion in the radial direction is of the order of 5-10 km s⁻¹, as derived by ob-

servations of e.g. Sanders, Solomon & Scoville (1984) in the Milky Way. In external galaxies, gas velocity dispersions obtained by Dickey, Hanson, & Helou (1990) and Boulanger & Viallefond (1992) span a similar range of values and they present rather flat profiles, i.e. independent of radius (except in the inner parts of the disks where they increase, but by a factor never exceeding ~ 2). On theoretical grounds the gas velocity dispersion is expected to vary little in self-regulated disks (Silk 1997). In that case, one obtains for disks with flat rotation curves : $\Sigma_{CRIT} \propto \kappa \propto R^{-1}$. Since this gradient of Σ_{CRIT} is shallower than the observed decline of the gas surface density, it is expected that $Q > 1$ at some “cut-off” radius, resulting naturally in a threshold of the SFR.

These ideas were studied in a seminal paper by Kennicutt (1989), with a sample of 15 (mostly late type) spirals. By using a constant gas velocity dispersion $\sigma_{GAS} = 6 \text{ km s}^{-1}$ he found that star formation declines rapidly in disk regions with $Q > 1.6$, i.e. for $\Sigma_{GAS} < 0.6 \Sigma_{CRIT}$. He also found that Q varies little within the star forming disk, an indication of self-regulating star formation.

Wang & Silk (1994) proposed to take into account the stellar contribution to the instability by rewriting the critical density as:

$$\Sigma_{CRIT} = \gamma \frac{\kappa \sigma_{GAS}}{\pi G}, \text{ with } \gamma = \left(1 + \frac{\Sigma_* \sigma_{GAS}}{\Sigma_{GAS} \sigma_*}\right)^{-1} \quad (6)$$

where Σ_* and σ_* are, respectively, the stellar surface density and the radial stellar velocity dispersion.

In the rest of Sec. 3 we study the instability criterion of equation 3 for galactic disks by using both definitions (4) and (6) for Σ_{CRIT} . In the former case, we adopt a constant value $\sigma_{GAS} = 6 \text{ km s}^{-1}$ for the gas velocity dispersion. In the latter, a knowledge of the radial stellar velocity dispersion is also required.

As shown by Bottema (1993), the radial stellar velocity dispersion of a disk is exponentially decreasing with the galactocentric radius; the corresponding scalelength is equal to twice the one observed in the B-band:

$$\sigma_*(R) = \sigma_0 \exp(-R/2h_B) \quad (7)$$

Moreover, Bottema (1993) showed that the value of the radial stellar velocity dispersion at one scalelength is comparable to the vertical stellar velocity dispersion at the centre of the galaxy. He also showed that the stellar velocity dispersion in a galactic disk is correlated with its rotational velocity V_C (Fig. 6). We computed a simple fit to his data (for the more reliable inclined galaxies) to obtain:

$$\sigma_*(R = h_B) [\text{km s}^{-1}] = -4.3 + 0.3 V_C [\text{km s}^{-1}] \quad (8)$$

i.e. the velocity dispersion of the stellar component is $\sim 1/3$ of the rotational velocity of the disk. In the same figure we display the recent data obtained by Vega Beltrán et al. (2001) concerning the kinematics of 20 disc galaxies. Despite some scatter, these data confirm the trend found by Bottema (1993). For 8 galaxies of our sample, central dispersion velocities are given by McElroy (1995). Assuming the same radial dependence as in Equ. 7, we computed the corresponding dispersion at one scalelength and plotted it also in Fig. 6; the results for the disks of our sample are clearly in agreement with the aforementioned trend. We are using then in the following these stellar velocity dispersions to calculate the value of Σ_{CRIT} , according to Equ. 6

3.2 Application to the Milky Way

Before studying the above stability criteria with our sample of disk galaxies, we present in Fig. 7 an application to the Milky way disk. In the upper panel we show the observed profiles of the total gas surface density ($H_2 + \text{HI}$, increased by 40% to include He contribution), the stellar profile (exponential, with scalelength of 2.5 kpc and normalised to $42 \text{ M}_\odot/\text{pc}^2$ in the solar neighborhood), and the profile of the stellar radial velocity dispersion, calculated according to the prescriptions of the previous paragraph and Bottema's (1993) data, by combining equations 7 and 8. In the middle panel, we show the profile of the ratio of the gas surface density to the critical density, which is calculated either by Eq. 4 (i.e. by taking into account only the gas velocity dispersion, assumed here to be 6 km s^{-1} at all radii) or by using Eq. 6 (i.e. by taking into account both the gaseous and the stellar components).

It can be seen that in the former case, the ratio

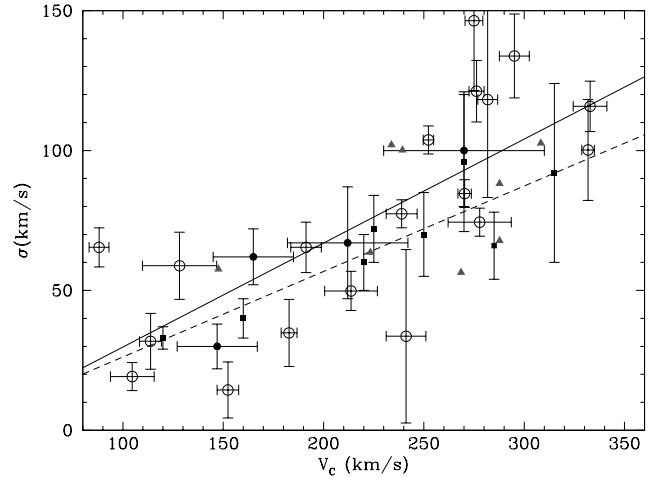


Figure 6. The radial stellar velocity dispersion at one scalelength for the inclined discs (filled squares) and the vertical one at $R=0$ for the face-on discs (filled circles) of Bottema (1993). Open circles are the recent data of Vega Beltrán et al. (2001). The dashed and solid lines show respectively a simple fit to the data of Bottema (1993) and Vega Beltrán et al. (2001). The triangles correspond to galaxies of our sample for which a velocity dispersion is given in McElroy (1995)

$\Sigma_{GAS}/\Sigma_{CRIT}$ remains roughly constant at an average value of ~ 0.65 , between 4 and 14 kpc, i.e. in a large part of the star forming disk; this value is very close to the value of 0.69 ± 0.20 that Martin & Kennicutt (2001) found as defining the SFR threshold in their sample of spiral galaxies (also shown as grey shaded area in Fig. 7). However, in the inner disk, i.e. in the “molecular ring” where most of the star formation activity is concentrated, the values of $\Sigma_{GAS}/\Sigma_{CRIT}$ are *below* the threshold found by Martin & Kennicutt (2001). The situation improves if the stellar radial dispersion profile is taken into account (*solid curve* in the middle panel of Fig. 7). Since, in the molecular ring one has $\Sigma_* \Sigma_{GAS} \sim 10$ and $\sigma_{GAS} \sigma_* \sim 0.1$, the resulting value of γ (Equ. 6) is $\sim 1/2$ and $\Sigma_{GAS}/\Sigma_{CRIT}$ increases in the inner Galaxy, up to the level of ~ 1 in the molecular ring.

In the lower panel of Fig. 7 we present the SFR profile of the Milky Way (normalised to the solar neighborhood SFR value), as given by various tracers (see Boissier & Prantzos 1999 for references to original data). It can be seen that the outer radius of the SFR profile of the Milky Way coincides with the radius of a steep decline in the $\Sigma_{GAS}/\Sigma_{CRIT}$ profile; this conclusion is valid for both ways of calculating Σ_{CRIT} .

To summarise, the Milky Way data

(i) support the idea of large scale star formation according to the Toomre instability criterion of Eq. (2), since the value of $\Sigma_{GAS}/\Sigma_{CRIT}$ is \sim constant across the star forming disk,

(ii) are consistent with the Martin & Kennicutt (2001) data for a threshold of star formation in external spirals (at a value of $\Sigma_{GAS}/\Sigma_{CRIT} \sim 0.7 \pm 0.2$ in most of the star forming disk) and

(iii) favor the idea that the stellar component should also be used in the instability criterion (at least in the inner

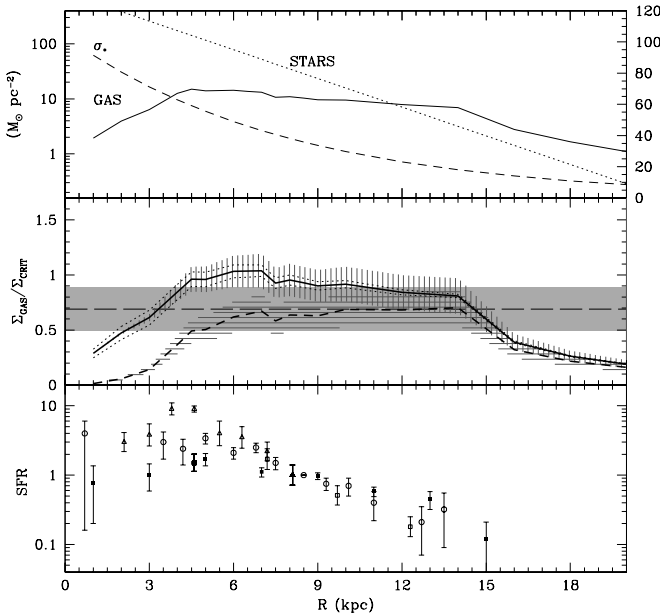


Figure 7. Gas, stars and star formation in the Milky Way disk. Upper panel: observed profiles of the total gas surface density (solid curve, H_2+HI , increased by 40% to include He contribution, the H_2 being derived from CO with a metallicity-dependent conversion factor), the stellar profile (dotted curve exponential, with scalelength of 2.5 kpc and normalised to $42 M_\odot/pc^2$ in the solar neighborhood), and the stellar radial velocity dispersion (dashed curve, calculated according to equations 7 and 8, in $km\ s^{-1}$ as indicated on the right axis). Middle panel: profile of the gas surface density to the critical density for two cases: first (dashed curve within horizontally hatched area, indicating the uncertainties on gas values), by using Eq. 4 for Σ_{CRIT} (i.e. by taking into account only the gas velocity dispersion, assumed here to be $6\ km\ s^{-1}$ at all radii); secondly (solid curve within vertically hatched area, indicating the uncertainties on gas values) by using Eq. 6 for Σ_{CRIT} (i.e. including the contribution of the stellar disc to the instability criterion). The shaded area indicates the value 0.69 ± 0.20 that Martin & Kennicutt (2001) found for the star formation threshold in their sample of galactic disks. Bottom panel: SFR profile in the Milky Way (from various tracers), normalised to its value in the Solar Neighborhood.

disk). This confirms the results of Wang and Silk (1994) who proposed this idea and tested it in the Milky Way.

Unfortunately, the situation with the other disks of our sample is not as clear-cut.

3.3 Thresholds for SF in galactic disks?

Figure 8 shows the profiles of the ratio $\Sigma_{GAS}/\Sigma_{CRIT}$ for the galaxies for which we have all the required information. The ratio was computed through equations 4 (circles) and 6 (squares). The epicyclic frequency was computed by adopting the analytical rotation curve of Equ. 2 (filled symbols), which was derived analytically. For seven galaxies, the high resolution rotation curves of Sofue et al. (1999) were also used and numerically derived, with very similar results (see Fig. 8, open symbols); an exception was the case of NGC 5194, in reason of its peculiar rotation curve. The absence

of difference between the two computations shows that the details of the rotation curve affect only little the critical density, compared to other quantities.

When the critical density is computed with only the gaseous component (Equ. 4), the disks are often found to be sub-critical over large intervals of their radial extent. Eight of the galaxies of our sample (2903, 2403, 4258, 3031, 4571, 4501, 4654, 4651) are found to be subcritical with respect to the average threshold value of $\Sigma_{GAS}/\Sigma_{CRIT}=0.69 \pm 0.20$ found by Martin and Kennicutt (2001); the gas density is substantially lower than the critical value even in regions with intense observed star formation. The rest of our sample is equally divided between critical (2541, 5194, 4321, 4713) and over-critical galaxies (925, 4254, 4303, 4654); in the latter case the value of $\Sigma_{GAS}/\Sigma_{CRIT}$ is considerably larger than the threshold value of Martin & Kennicutt (2001). We note that all three cases are encountered with similar frequencies in isolated and Virgo spirals, i.e. the environment does not seem to play a role in the overall disk instability.

As in the case of the Milky Way, including the stellar component in the instability criterion (Equ. 6) leads to larger values of the ratio $\Sigma_{GAS}/\Sigma_{CRIT}$ in the whole disk. Only two disks still remain sub-critical with the modified criterion (3031, 4571) and only marginally so. In a few cases (4303, 4654) the modified values of $\Sigma_{GAS}/\Sigma_{CRIT}$ are three times larger than the threshold value found by Martin & Kennicutt (2001).

The average value of $\Sigma_{GAS}/\Sigma_{CRIT}$ at the outer edge of the star forming disks in our sample is 0.50 when only the gaseous component is included in the instability criterion and 0.73 when the stellar component is also included. Due to the large variations between the values of $\Sigma_{GAS}/\Sigma_{CRIT}$ in our disks, we find a large dispersion in the average threshold values : ± 0.33 in the former case and ± 0.38 in the latter, i.e. almost the double of the dispersion found by Martin & Kennicutt (2001).

We found that the evaluation of the H_2 profile in the outer parts of the galaxies is crucial for the derivation of $(\Sigma_{GAS}/\Sigma_{CRIT})_{thres}$. When the H_2 surface density profile is not extrapolated beyond the last observed point (i.e. assuming that no molecular gas is present beyond that point), we obtain a threshold value $(\Sigma_{GAS}/\Sigma_{CRIT})_{thres}=0.32 \pm 0.16$. When a fit is performed to the H_2 profile, and extrapolated beyond the last observed point, the result is the previously mentioned 0.50 ± 0.33 ; this is in agreement with the value of 0.69 ± 0.2 of Martin & Kennicutt (2001) who used the same assumption.

In conclusion, contrary to the case of the Milky Way disk, our analysis of external spirals does not find evidence supporting the application of the (original or modified) Toomre criterion for large scale star formation; it is true, however, that the inclusion of the stellar component in the instability criterion makes most of our disks overcritical according to that criterion. Also, it is worth noting that stars are very often present beyond the threshold radius, as it can be seen on the photometric profiles (Fig. 2), suggesting that some star formation must have occurred in those regions in the past.

Our conclusions differ from the ones of Martin & Kennicutt (2001) despite the fact that we have a large number of galaxies in common (13 out of 16 in our sample). In their larger sample of 32 disks they find only seven sub-critical

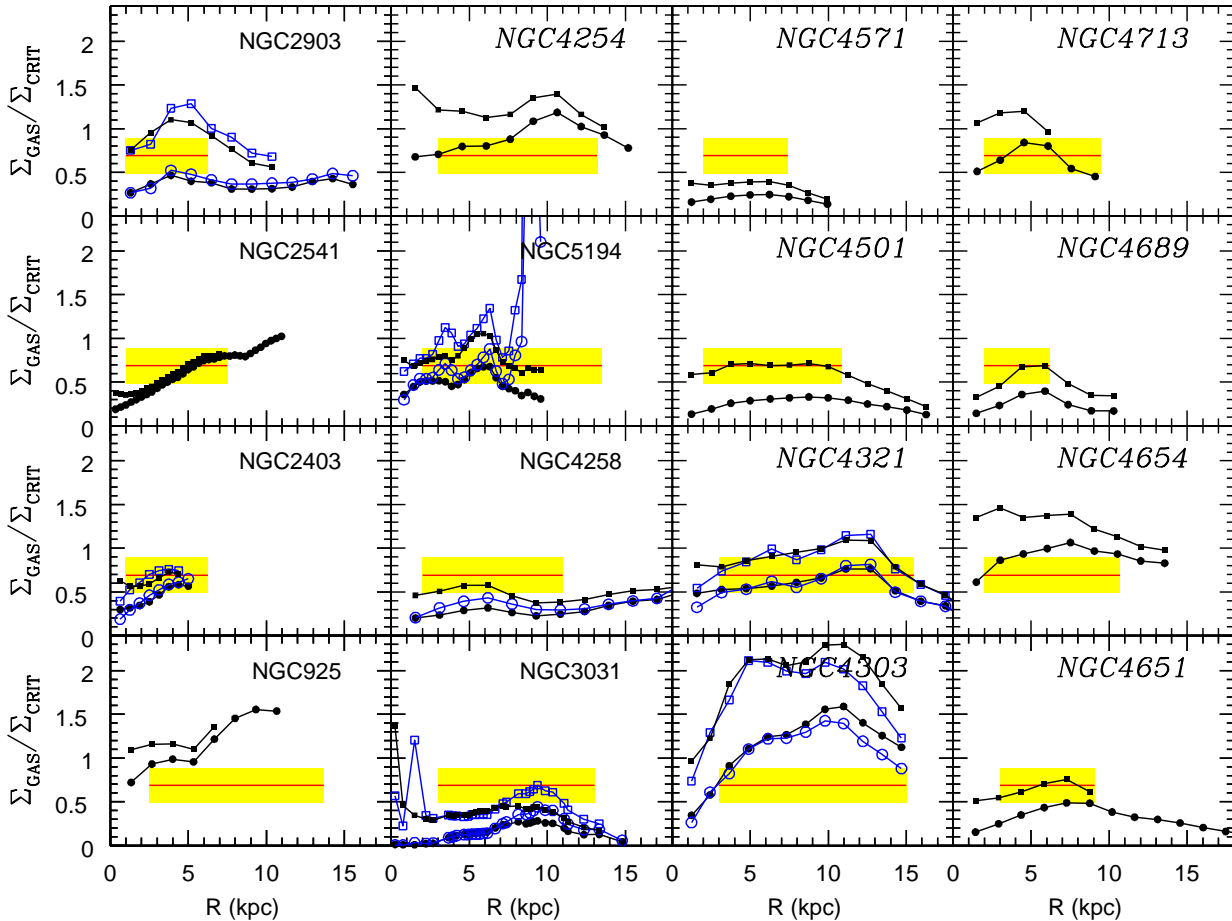


Figure 8. Ratio of the gas density to the critical density, when gas only is taken into account in the instability criterion (filled circles) and when the stellar density is taken into account (filled squares); the epicyclic frequency was computed with the analytical rotation curve of Eq. 2 (section 2.7). When a high resolution rotation curve was available (Sofue et al. 1999), the epicyclic frequency was numerically derived and the corresponding results are indicated by open circles and squares, respectively. The horizontal line and the shaded area at 0.69 ± 0.2 correspond to the threshold values for star formation found by Martin & Kennicutt (2001); the inner limit of that line corresponds to the bulge/disk limit and the outer one to the observed threshold in star formation (see Sec. 2.4). Galaxies with names in *italics* belong to the Virgo cluster.

(i.e. 22 %), whereas we find that eight of our 16 disks are sub-critical. Among the galaxies in common, four were found to be subcritical in our study but not in Martin & Kennicutt (2001): NGC 2903, 4501, 4651, 4689. Inspection of figure 5 shows that the molecular gas represents a significant fraction of the total amount of gas over a large fraction of the disc within the threshold radius for these galaxies. At the same time, Fig. 1 indicates a quite large effect of the metallicity on the determination of the H₂ surface density: with a constant conversion factor, Martin & Kennicutt overestimate the amount of H₂ with respect to us. The differences in the fraction of sub-critical disks and in the value of $(\Sigma_{GAS}/\Sigma_{CRIT})_{thres}$ in our study and theirs mainly reflect differences in the evaluation of the conversion from CO to H₂.

We note that recently Wong & Blitz (2002) reached similar conclusions with us, concerning the validity of the Toomre criterion. Their analysis of a different sample of galaxies failed to show a clear relationship between the Q

value and large scale star formation. They note, however, that $Q \sim 1$ is often observed in galactic disks, while two disks with high Q values (sub-critical) have small gas fractions; they suggest then that Q is actually a measure of the gas fraction in the disk and they support their suggestion with a rather qualitative analysis (see their Sec. 5.3).

We have used our detailed stellar and gas profiles to derive corresponding gas fraction profiles, computed as $\Sigma_{GAS}/(\Sigma_{GAS} + \Sigma_*)$, for all the galaxies of our sample and we plotted the Q values as a function of the gas fraction (Fig. 9). If Wong & Blitz (2002) were right, we would expect to find an anti-correlation between Q and the gas fraction, large values of Q corresponding to low gas fractions. On the contrary, our results suggest no correlation between low values of the gas fraction and sub-critical disks: Nine of our disks are indeed sub-critical at a gas fraction of ~ 0.1 , as argued by Wong and Blitz (2001), but seven are clearly critical. Also, we have several galaxies which are sub-critical at gas fractions ~ 1 , whereas they should be critical according to Wong

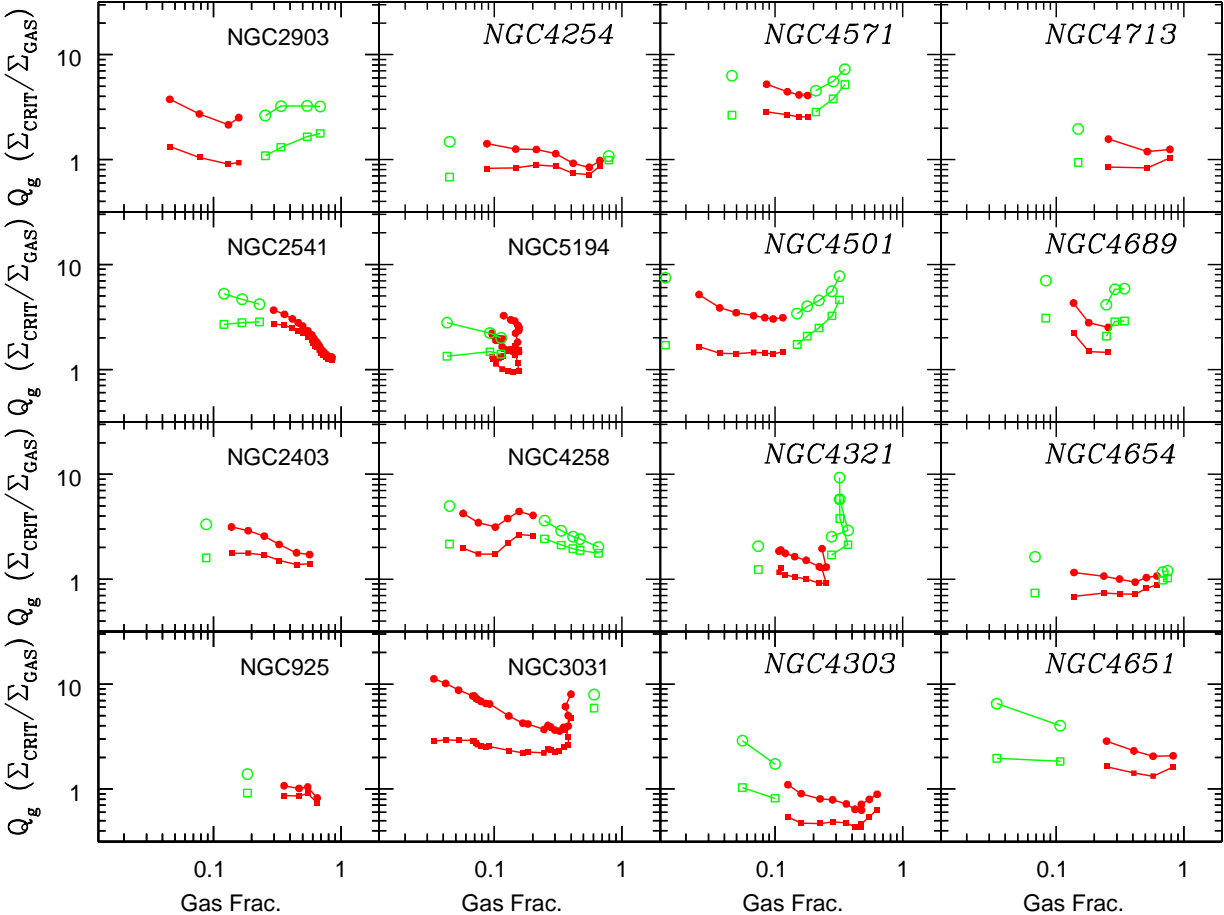


Figure 9. Ratio of the gas density to the critical density as a function of the gas fraction for all the disks of our sample, when gas only is taken into account in the instability criterion (circles) and when the stellar density is taken into account (squares). Filled symbols correspond to regions of active star formation (i.e. inside the shaded bars of Fig. 8) and open symbols to regions outside.

& Blitz (2001). Thus, our analysis does not support the idea that Q is a measure of the gas fraction in the disk.

4 THE STAR FORMATION LAW

4.1 Star formation vs gas amount

A comprehensive review of our current (non) understanding of large scale star formation in galaxies has been recently presented by Elmegreen (2002), who also provides an extensive reference list on the subject.

Intuitively, star formation should be associated to the molecular content of a galaxy, rather than to the neutral gas amount. Such a correlation has indeed been claimed to be observed in spirals by Young and collaborators (e.g. Rownd et al. 1999), under the assumption of a constant conversion factor of CO to H₂. Similar conclusions were reached by Boselli et al. (1995), who showed that the molecular mass follows quite closely the star formation rate in luminous spirals; the galaxies of their sample display similar metallicities and the assumption of a constant conversion factor is then justified. However, it was argued by Boselli et al. (1995) that

the scatter obtained for less luminous galaxies could be due to variations in the conversion factor. Boselli et al. (2002) showed recently that the conversion factor depends indeed on the physical properties of the galaxy. Once a metallicity-dependent conversion factor is adopted, a good correlation is observed between H₂ and the star formation rate.

As discussed in Sec. 2.3 we adopted in this paper a metallicity-dependent conversion factor to compute the densities of H₂ within the disks of our sample. It can be seen on Fig. 10 that the resulting azimuthally averaged molecular gas surface density presents a better correlation with the star formation rate density than the neutral gas (left and middle panels, where the H₂ and SFR profiles have been smoothed to the HI resolution, and corrected for the He fraction by multiplying them by 1.4). The good agreement correlation between H₂ and the star formation rate in our analysis of azimuthally averaged quantities corroborates the findings of Boselli et al. (2002) concerning global quantities of the disks.

Instead of thinking the star formation process as a sequence (neutral gas towards molecular gas towards stars), one may consider it as the result of dynamical processes

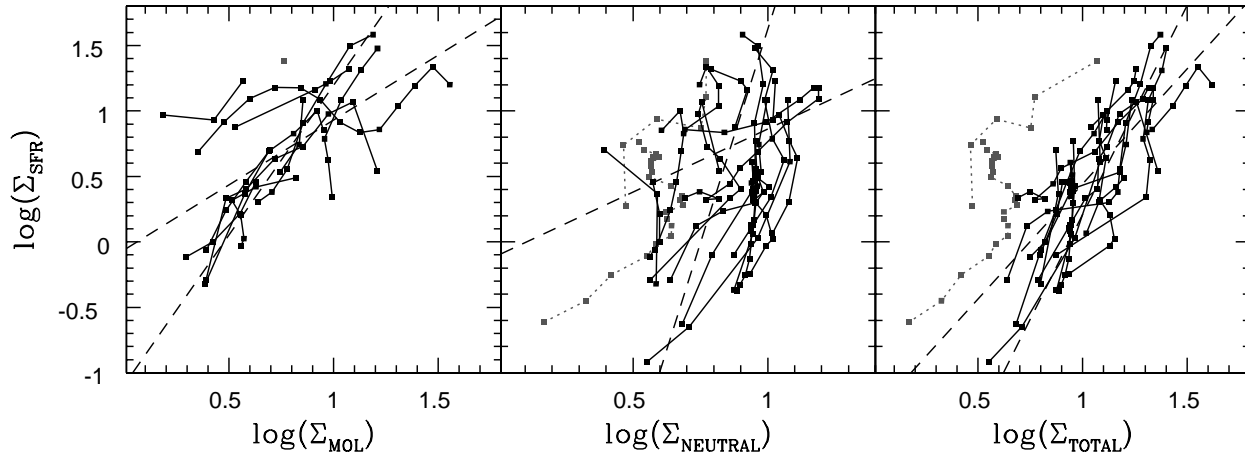


Figure 10. Star formation rate density as a function of molecular gas density (*left*), neutral gas density (*middle*) and total gas density (*right*); units are $M_{\odot} \text{pc}^{-2} \text{Gyr}^{-1}$ for the SFR and $M_{\odot} \text{pc}^{-2}$ for the gas (where the He fraction has been accounted for). The data are smoothed to the HI resolution. The *solid curves* connect points within the same galaxy. The *dashed lines* are the two regression fits in each case (see text); the galaxies NGC3031 and NGC4258 (indicated by the *dotted curves*) are excluded from the fit.

involving the totality of the gas density. In that case, a better correlation should be found between the star formation rate and the total gas density rather than either the molecular or the neutral component. Indeed, since Schmidt (1959), there has been evidence that the star formation rate density (Σ_{SFR}) is related to the total gas density (Σ_{GAS}) (e.g. Kennicutt 1998a):

$$\Sigma_{SFR} = \alpha \Sigma_{GAS}^n \quad (1 < n < 2). \quad (9)$$

Basic models based on self-gravitating discs can produce such a “Schmidt law” (e.g. Kennicutt 1998b). The right panel of Fig. 10 displays a reasonably good correlation between the star formation rate and the gas density for most of the galaxies of our sample. Two galaxies which are rather peculiar can be easily identified on this plot. One of them is NGC 3031 which has a low gas content but a high star formation rate, especially in its inner part; this galaxy is forming stars despite being sub-critical (Fig. 9). The other is NGC 4258 and displays a normal gas content but a larger efficiency to form stars than all the other galaxies in our sample.

We stress that the correlations displayed in Fig. 10 concern *azimuthally averaged* quantities, whereas Boselli et al. (2002) or Kennicutt (1998a) studied such correlations between global quantities or averaged over the whole disk (inside the optical radius).

The Schmidt law is the most widely used, but other semi-empirical “recipes” of star formation have been suggested for galactic disks (and implemented in relevant models).

Ohnisi (1975) suggested that star formation is enhanced by the passage of spiral density waves with a frequency $\Omega(R) - \Omega_P$, where $\Omega(R)$ is the galaxy’s rotational frequency at radius R and Ω_P the frequency of the spiral pattern; for $\Omega(R) \gg \Omega_P$ this leads to a star formation rate $\text{SFR} \propto \Omega(R) \propto V(R)/R$, where $V(R)$ is the corresponding rotational velocity (see also Wyse & Silk 1989). According to

Larson (1988) the presence of the $\Omega(R)$ factor in the radial variation of the star formation rate could also be obtained if a self-regulation of star formation occurs such that $\Sigma_{GAS} \sim \Sigma_{crit}$. Kennicutt (1998a) has indeed found that the observed averaged (over the optical radius) densities of the star formation rate and the total gas density are related equally well either by a simple Schmidt law (Equ. 9) or by the form:

$$\Sigma_{SFR} = \alpha \Sigma_{GAS} / \tau_{DYN} \quad (10)$$

where $\tau_{DYN} \sim R/V(R)$ is the dynamical timescale at radius $R = R_{OPT}$.

In Boissier & Prantzos (1999), a “semi-theoretical” SFR deduced from those consideration was adopted:

$$\Sigma_{SFR} = \alpha \Sigma_{GAS}^n V/R, \quad (11)$$

(V being the rotational velocity, taken constant and equal to 220 km s^{-1} for the Milky Way). The index n was chosen to be $n=1.5$ on empirical basis (providing the observed relation between $\Sigma_{SFR}(R)$ and $\Sigma_{GAS}(R)$ and reproducing the observed abundance gradient). This theoretical star formation rate was adopted in subsequent models extended to all spiral galaxies, which reproduced successfully their global properties (Boissier & Prantzos 2000; Boissier et al. 2001) and their abundance and colour gradients (Prantzos & Boissier 2000).

Another star formation law, sometimes used in models of chemical evolution (e.g. Matteucci & Chiappini 2001) was suggested by Dopita & Ryder (1994) on the basis of an observed correlation between the stellar surface density (as traced by I-band photometry) and the star formation rate:

$$\Sigma_{SFR} = \alpha \Sigma_{GAS}^n \Sigma_T^m \quad (12)$$

where Σ_T is the total surface density (gas plus stars). Dopita & Ryder (1994) tested only indirectly this law (via a model, since they had no gas data available) and found it to be consistent with observations if $n + m$ is between 1.5 and

2.5. They also presented a model of stochastic self-regulating star formation, predicting $n=5/3$ and $m=1/3$, values that are in agreement with their empirical findings.

4.2 Empirical determination of SF parameters

We tested the three SF laws of equations 9, 11 and 12 with our data (with all the data being smoothed to the HI resolution). The gas profile was multiplied by a factor 1.4 to take into account the He contribution. The H₂ data were extrapolated assuming an exponential profile (see below for a discussion of this assumption). Equ. 11 requires the rotational velocity $V(R)$, that we simply approximated by the analytical rotation curve of Equ. 2. For Equ. 12 we need an estimate of the total surface density, that is of the stellar density; the photometric H band profiles, barely affected by dust extinction, were used for that purpose, assuming the same mass to luminosity ratio (M_*/L_H) as in Boissier et al. (2001).

Fig. 11 shows our data plotted in the plane Σ_{GAS} vs Σ_{SFR} (top, testing Equ. 9), in the plane Σ_{GAS} vs $\Sigma_{SFR} \times R/V(R)$ (middle, testing Equ. 11) and in the plane Σ_{GAS} vs $\Sigma_{SFR} \times \Sigma_{GAS}^n \Sigma_T^{-0.61}$ (bottom, testing Equ. 12). In the last case, the best-fit value for the second parameter m was adopted for the figure (i.e. the one minimising the χ^2 for the SFR).

The points corresponding to a single galaxy are connected by a grey line. The dashed lines show simple least square fits, one minimizing the deviation on the SFR density, and one on the gas surface density (the difference between the indexes in each case gives an idea of the dispersion of the relation). Since we are searching for the “best fit law” of the SFR, we will adopt for the discussion the first of these two fits.

The dotted lines correspond to NGC3031 and NGC4258. The latter is obviously an outlier, having quite low gas density but relatively high SFR (see Fig. 5) and we do not consider it in the fits; note that high resolution CO data for this galaxy differs from the low resolution ones (see section 2.3). We also ignored NGC3031, because its gaseous profile (HI and total) is very atypical (see Fig. 5). It is the only object in our sample with a low gas density over the whole disc. NGC3031 is indeed among the more sub-critical discs of Martin & Kennicutt (2001).

One would expect that the outlying or peculiar galaxies in Fig. 11 (as well as in Figs. 8,9,10) could be systematically associated to the cluster environment, HI-deficient objects, or have a peculiar morphology. We do not find obvious trends in our small sample, however the analysis of Gavazzi et al. (2002) on integrated quantities has shown that cluster HI-deficient galaxies have, on average, lower star formation activities than their field counterparts.

For a simple Schmidt law (Equ. 9), the least-square fit gives an index $n \sim 2$, steeper than the 1.4 suggested by Kennicutt (1998b) or the 1.3 ± 0.3 of his earlier work (Kennicutt, 1989). When a dynamical factor is introduced (Equ. 11), we obtain $n \sim 1.5$, steeper again than the slope $n \sim 1$ found by Kennicutt (1998b). However the introduction of Ω in both studies acts in the same direction: it reduces the value of n .

The differences between our results and those of Kennicutt (1998b) may be due to several reasons: i)

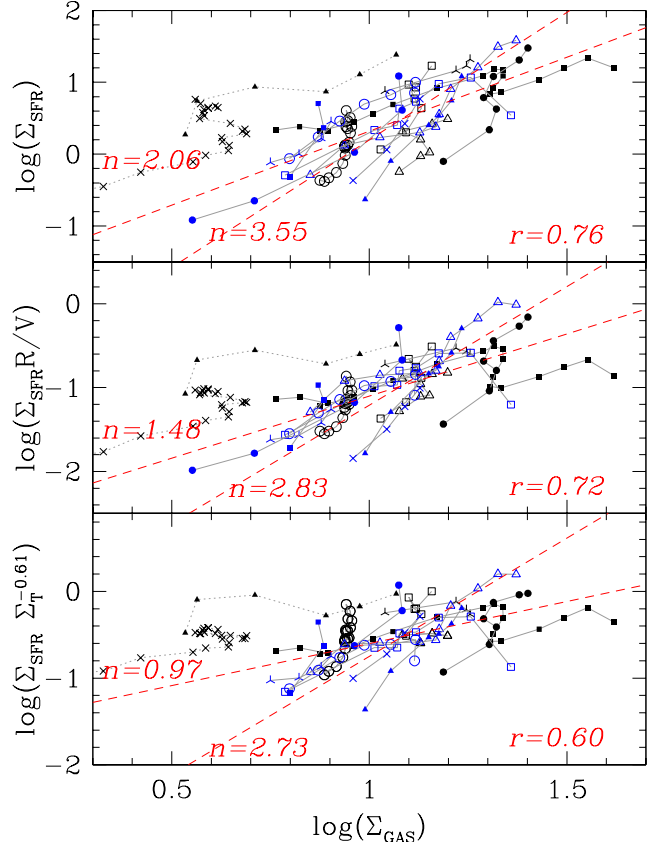


Figure 11. Test of various star formation laws. *Top*: gas surface density vs Star Formation Rate surface density (testing the standard Schmidt law, Equ. 9). *Middle*: gas density vs $\Sigma_{SFR} \times R/V(R)$ (testing Equ. 11). *Bottom*: gas density vs $\Sigma_{GAS}^n \Sigma_T^{-0.61}$ (testing a Dopita- Ryder law, Equ. 12, with the best value of the second parameter $m=0.61$). The grey lines connect points of the same galaxy (the dotted lines correspond to NGC4258 and NGC3031, not considered in the fits, see section 4.2). Different symbols are used for different galaxies. The dashed lines show two fits, one minimizing deviations on Σ_{SFR} (the one that should be used for a determination of the SFR parameters) and one minimizing deviations on Σ_{GAS} . The corresponding index n is indicated for each one of them and is also reported on Table 3. The correlation coefficient (r) is indicated in the right-bottom part of each panel.

Kennicutt (1998b) uses surface densities averaged within the optical radius, i.e. he includes the bulge region (while we only study the star forming disk) and in some cases he also includes some gas located beyond the threshold radius (while we work on radial profiles within the radial range of interest); ii) The law obtained by Kennicutt (1998b) was established on a large range of gas surface density (an astonishing factor 10^5) by introducing in the sample star-burst galaxies; however, for normal discs only, his analysis also showed a large dispersion of the index n , with values ranging from 1.29 for a standard least square to 2.47 for a bivariate least-square regression (for a standard Schmidt law, Equ. 9). The corresponding values in our case are respectively 2. and 2.6. iii) We use a conversion factor between CO and H₂ that depends explicitly on the metallicity, while he adopts a con-

Table 3. Slopes of the star formation laws under two different assumptions on the molecular content at large radii. The values of the exponent n are given for the two regression lines in each case. For the Dopita-Ryder law, the “best-fit” value of the second parameter (m) was assumed. Note that adopting a flat rotation curve barely affects the values of n for the $\Sigma_{GAS}^n \Omega$ law.

Σ_{SFR}	No H ₂ extrapolation	H ₂ extrapolation
$\alpha \Sigma_{GAS}^n$	1.96 (3.1)	2.06 (3.55)
$\alpha \Sigma_{GAS}^n \Omega$	1.38 (2.52)	1.48 (2.83)
$\alpha \Sigma_{GAS}^n \Sigma_T^m$	1.00 (2.21) for $m=0.56$	0.97 (2.73) for $m=0.61$

stant conversion factor. This important point also applies to the comparison of our work and the one of Kennicutt (1989), also based on radial profiles of spiral galaxies. iv) The galaxy sample is different; it is obvious from Fig. 11 that star formation in galaxies does not obey a well defined relation but present a large scatter around an average one. The SFR law can then be defined only in a statistical sense, and since the number of galaxies for which such studies can be done is still small, it is understandable that studies with different samples produce different results.

Wong & Blitz (2002) used a small sample of 7 galaxies only, but with higher spatial resolution. Assuming a uniform model of extinction (comparable to the present work) they found for the simple Schmidt law a value of $n=1.1$, i.e. they found a relation less steep than both us and Kennicutt (1998b). On the other hand, assuming a dependence of extinction on the gas column density they found $n=1.7$. They also found that a SFR of the form $\Sigma_{GAS} \Omega$ is compatible with their data, but only if an important radially dependent extinction is assumed. However, they did not attempt to fit a law of the form of Equ. 11.

The differences between our work and Wong & Blitz (2002) may result from: i) The small statistics (as previously discussed); ii) The fact that the galaxies of Wong & Blitz (2002) are selected to be bright in CO, i.e. H₂-rich, which may introduce some bias in the sample, as these authors also acknowledge; iii) The sensitivity of the obtained index n to the assumed extinction gradient, which is difficult to evaluate since it depends also on the abundance gradient, and since the observed scatter at a given radius is stronger than that gradient (Martin & Kennicutt 2001). iv) The assumption of a constant conversion factor of CO to H₂.

Finally, we tested the SF law proposed by Dopita & Ryder (Equ. 12) with the sub-sample for which the stellar density profile is available from H-band photometry. A simple least square fit (minimizing the deviation on Σ_{SFR}) to our data leads to $n \sim 1$ and $m \sim 0.61$, substantially different from the values 5/3 and 1/3 obtained by Dopita & Ryder (1994).

The results presented in Fig. 11 are obtained by adopting the analytical rotation curve of Equ. 2 and an extrapolation of the molecular gas profile, as described in Sec. 3. To test the effect of these assumptions, we did the same work assuming that there is no molecular gas beyond the last CO detection point. The difference in the slopes of the relationships are presented in Table 3.

The differences are relatively modest, contrary to what occurred for the threshold, since the fits are essentially deter-

mined by the data concerning the main body of the molecular disk.

Adopting a flat rotation curve instead of the analytical rotation curve of Equ. 2 leads also to small differences: we obtain a slightly lower slope (1.28 in the case of no H₂ extrapolation and 1.32 in the case of H₂ extrapolation) for a flat rotation curve than with the analytical rotation curve (respectively 1.38 and 1.48).

In conclusion, the SF laws that we obtained depend only weakly on assumptions concerning the rotation curve and the molecular gas profile in the outer disk.

4.3 Application to the Milky Way

In the previous section, we determined the parameters of three widely used star formation laws (equations 9, 11, 12) by means of our galaxy sample. As in the case of the SF threshold (see Sec. 3.2), it is interesting to see how the resulting SF laws match the star formation data of the Milky Way disk.

Using the well known gaseous and stellar radial profiles of the Milky Way and a flat rotation curve ($V(R)=220$ km s⁻¹), we calculated the corresponding SF profiles; the results are displayed in Fig. 12, respectively for the simple Schmidt law (*dotted curve*), the Schmidt law modified by the dynamical factor V/R (*short-dashed curve*) and the Schmidt law modified by the stellar density (*long-dashed curve*). We compare the results to the SF radial profile of the Galaxy, as estimated through various tracers (Lyne et al. (1985), Gusten & Mezger (1983), Guibert et al. (1978), and Case & Bhattacharya (1998)). Note that the observations were scaled to the value of the SFR in the solar neighborhood which has its own uncertainty; the box in the center of the figure indicates the range of its possible values (Rana 1991).

The three SF laws produce quite similar results in the range 4-18 kpc, i.e. in the whole radial extent of the disk. The pure Schmidt law fails considerably in the inner disk (inside 3 kpc), since the low amounts of gas there do not allow it to reproduce the relatively high values of observed SFR. All three laws give satisfactory results in the 4-15 kpc range, while the modified Schmidt laws fit the observations also in the inner disk; however, due to several complications that might arise in that region (i.e. role of the bar in the star formation) the “success” of the modified Schmidt laws in that region should not be considered as a “proof” of their validity.

In summary, data for the Milky Way disk are compatible with all three SF laws that we empirically determined in the previous section. Only a consistent application of those SF laws in a chemical evolution model of the Milky Way could (perhaps) favour one of these SF laws over the others, by comparison to as many observed radial profiles as possible (e. g. chemical and photometric profiles, as in the work of Boissier & Prantzos 1999 for the gaseous, chemical and photometric profiles of the MW disk). We note, however, that in practice, even this test may not be conclusive, because of the poorly known radial and temporal dependence of the gas infall rate on the disk. Gaseous infall is indeed required, at least in the solar neighborhood to account for the so-called “G-dwarf problem” (e.g. Pagel 1997 and references therein).

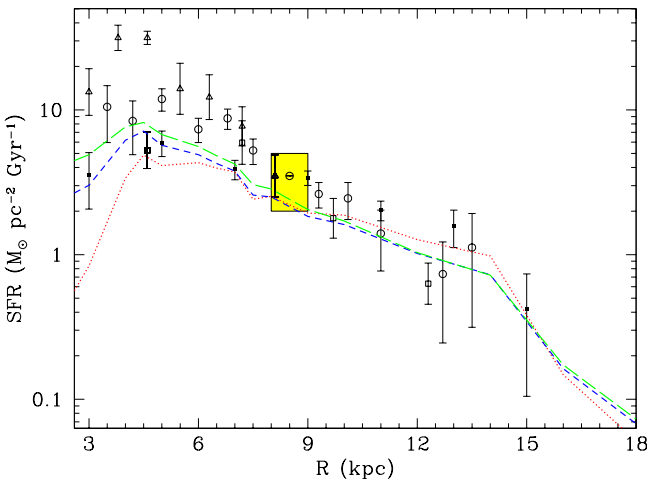


Figure 12. Application of the three SF laws obtained in section 4.2 (pure Schmidt: *dotted*, Schmidt modified by rotation: *short-dashed*, and Schmidt modified by stellar density: *long dashed*). They are compared with various SF tracers in the disk of the Galaxy (see section 4.3 for References).

5 SUMMARY

In this paper we present a detailed study of the properties of star formation in disk galaxies. We use an extended data set, consisting of (azimuthally averaged) radial profiles of stellar and gaseous (atomic and molecular) surface densities, of star formation rates and rotation curves. The molecular gas is derived from CO with a metallicity dependent conversion factor for the first time in this kind of study. These data allow questions related to the star formation rate and to the existence of a star formation threshold in galactic disks to be studied. Our sample comprises 16 disk galaxies, about half of which belong to the Virgo cluster.

Our results may be summarised as follows:

The existence of star formation threshold in our disks was studied by using the Toomre (1964) instability criterion and using either the gaseous component alone or both the gaseous and stellar components in the definition of the instability parameter Q . In the latter case, the profile of stellar velocity dispersion is also required and we calculated it for our disks based on the observations of Bottema (1993). We also used both analytical and observed rotation curves for the evaluation of Q .

We find that only half of our sample galaxies are over-critical (i.e. locally unstable and prone to form stars) when the gaseous component alone is taken into account, even in disk regions where observations indicate that vigorous star formation is taking place. Including the stellar component improves substantially the situation, since only two disks remain sub-critical then (and only marginally so).

These results refer to an average value of the instability parameter $Q=0.70\pm 0.20$ (i.e. slightly lower than unity), as observationally determined by Martin & Kennicutt (2001) with a larger disk sample (32 galaxies). Our own Q value, determined at the termination of the SF profile, is similar to the above value when the stellar component is included and slightly lower when it is ignored (0.71 and 0.5, respectively). However, in both cases, corresponding uncertainties

are larger than found by Martin & Kennicutt (0.38 and 0.33, respectively, compared to 0.20 in their case).

We find that the instability criteria apply fairly well to the Milky Way disk, where Q values are systematically ~ 0.7 when the gaseous component alone is used and $\sim 0.9-1$ when the stellar component is also included. We find it encouraging that the galaxy with the best defined profiles shows such an exemplary behaviour. We think that the large dispersion in the Q values found in our sample result (at least partly) from systematic uncertainties in the various profiles entering the evaluation of Q . Among them, of crucial importance are: i) the conversion factor of CO emission to H_2 gas amount (we use a metallicity dependent conversion factor, unlike previous studies) and, even more so ii) the extrapolation of the H_2 profile beyond the last observed point. These factors explain to a large part the quantitative differences between our results and those of Martin & Kennicutt (2001) and Wong & Blitz (2002). In particular, our findings do not support the claim of Wong & Blitz (2002) that Q is actually a measure of the gas fraction in the disks.

In agreement with Wong & Blitz (2002) we find that the observed local (i.e. at a given radius) SF rate density correlates better with the total gas density or with the molecular gas density than with the neutral gas density. We analysed three local SF laws with our data: a pure Schmidt law $SFR \propto \Sigma_{GAS}^n$, a Schmidt law modified by the disk rotational frequency $SFR \propto \Sigma_{GAS}^n V(R)/R$, and a Schmidt law modified by the local surface density Σ_T : $SFR \propto \Sigma_{GAS}^n \Sigma_T^m$ (according to a suggestion by Dopita & Ryder 1994).

We find that the modified Schmidt laws do slightly better than the pure Schmidt law, as expected in view of their supplementary degrees of freedom. We also find a larger index n for the gaseous component than Kennicutt (1998), both for the pure Schmidt law and for the one modified by rotation (2 and 1.5, compared to 1.4 and 1, respectively). We note that Kennicutt's analysis included starbursts, so that his gas surface densities covered five decades in magnitude, instead of ~ 1.5 decade in our case; by limiting his analysis to the low surface density normal spirals, Kennicutt (1998) also found larger values of n , close to ours. Besides, his analysis concerned only averaged quantities over the galactic disks, whereas ours concerns azimuthally averaged quantities, a fact which certainly explains the largest dispersion and the poorest fits that we obtain. On the other hand, Wong & Blitz (2002) used only azimuthally averaged quantities in their study and found values of $n=1.1$ for a uniform extinction model and 1.7 for an extinction dependent on the column density in the case of the pure Schmidt law; the latter case corresponds more to our own results.

Again, we find that the three derived SF laws apply fairly well to the data of the Milky Way disk, although the pure Schmidt law fails in the inner Galaxy (where the situation is uncertain anyway, due to the poorly known role of the galactic bar). The exemplary behaviour of the Milky Way disk makes us think that (either it is exceptional or) a much more systematic work than this one could allow to determine much better the local properties of star formation in disks. Such a work should involve: a much larger number of (unperturbed) disks than used here; much more extended and detailed radial profiles, especially in the case of molecular gas (for instance the results of the recent BIMA survey, Regan et al. 2001); and, above all, a much better understand-

ing of the various systematic uncertainties of the problem, for instance concerning the absolute local values of the star formation rate and the role of non axisymmetric profiles.

REFERENCES

Adler D. S. , Westpfahl D. J. 1996, AJ, 111, 735
 Begeman K. G., 1987, Ph.D. thesis, Kapteyn Institute, (1987)
 Boissier S., Prantzos N., 1999, MNRAS, 307, 857
 Boissier S., Prantzos N., 2000, MNRAS, 312, 398
 Boissier S., Boselli A., Prantzos N., Gavazzi G. 2001, MNRAS, 321, 733
 Boselli A. , Gavazzi, G., 2002, A&A, 386, 124
 Boselli A., Gavazzi G., Lequeux J., Buat V., Casoli F., Dickey J., Donas J., 1995, A&A, 300, L13
 Boselli A., Tuffs R. J., Gavazzi G., Hippelein H., Pierini D., 1997, A&AS, 121, 507
 Boselli A., Gavazzi G., Franzetti P., Pierini D., Scodeggio M., 2000, A&AS, 142, 73
 Boselli A., Gavazzi G., Donas J., Scodeggio M., 2001, AJ, 121, 753
 Boselli A., Lequeux J., Gavazzi G., 2002, 384, 33
 Boselli A., Gavazzi G., Sanvito G., 2003, A&A, 402, 37
 Bottema R., 1993, A&A, 275, 16
 Boulanger F. , Viallefond F., 1992, A&A, 266, 37
 Braine J., Combes F., Casoli F., Dupraz C., Gerin M., Klein U., Wielebinski R., Brouillet N., 1993, A&AS, 97, 887
 Broeils A., van Woerden H., 1994, A&AS, 107
 Case G., Bhattacharya D., 1998, ApJ, 504, 761
 Chincarini G. , de Souza R., 1985, A&A, 153, 218
 Dickey J. M., Hanson M. M., Helou G., 1990, ApJ, 352, 522
 Distefano A., Rampazzo R., Chincarini G., de Souza R., 1990, A&AS, 86, 7
 Dopita M., Ryder S., 1994, ApJ, 430, 163
 Drozdovsky I. O., Karachentsev I. D., 2000, A&AS, 142, 425
 Elmegreen B. G., 2002, ApJ, 577, 206
 Feldmeier J. J., Ciardullo R., Jacoby G. H., 1997, ApJ, 479, 231
 Freedman W. et al., 2001, ApJ, 553, 47
 Garnett D., Shields G., Skillman E., Sagan S., Dufour R., 1997, ApJ, 489, 63
 Gavazzi G., 1987, ApJ, 320, 96
 Gavazzi G., Boselli A., Pedotti P., Gallazzi A., Carrasco L., 2002, A&A, 396, 449
 Gavazzi G., Boselli A., Donati A., Franzetti P., Scodeggio M., 2003, A&A, 400, 451
 Guhathakurta P., van Gorkom J. H., Kotanyi C. G., Balkowski C., 1988, AJ, 96, 851
 Guibert J., Lequeux J., Viallefond F., 1978, A&A, 68, 1
 Gusten R., Mezger M., 1983, Vistas astr., 26, 159
 Haynes M., Giovanelli R., 1984, AJ, 89, 758
 Huchtmeier W. K., Richter O.-G., 1989, A General Catalog of HI Observations of Galaxies. The Reference Catalog. (A General Catalog of HI Observations of Galaxies. The Reference Catalog, XIX, 350 pp. 8 figs.. Springer-Verlag Berlin Heidelberg New York)
 Jarrett T.H., Chester T., Cutri R., Schneider S., Huchra J., 2002, submitted to the AJ.
 Kennicutt R. C., 1989, ApJ, 344, 685
 Kennicutt R. C., 1998a, ARAA, 36, 189
 Kennicutt R. C., 1998b, ApJ, 498, 541
 Larson R. B., 1988, in NATO ASIC Proc. 232: Galactic and Extragalactic Star Formation, 459
 Lyne A., Manchester R., Taylor J., 1985, MNRAS, 213, 613
 Martin C., Kennicutt R., 2001, ApJ, 555, 301
 Matteucci F., Chiappini C., 2001, New Astronomy Review, 45, 567
 McElroy D. B., 1995, ApJS, 100, 105
 Nakai N., Kuno N., 1995, PASJ, 47, 761
 Nilson P., 1973, Uppsala general catalogue of galaxies, Acta Universitatis Upsaliensis. Nova Acta Regiae Societatis Scientiarum Upsaliensis - Uppsala Astronomiska Observatoriums Annaler, Uppsala: Astronomiska Observatorium Ohnisi T., 1975, Progress in Theor. Phys., 53, 1042
 Pagel B., 1997, Nucleosynthesis and Galactic Chemical Evolution (Cambridge: CUP)
 Pierini D., Gavazzi G., Boselli A., Tuffs R., 1997, A&AS, 125, 293
 Pisano D. J., Wilcots E. M., Elmegreen B. G., 1998, AJ, 115, 975
 Prantzos N., Boissier S., 2000, MNRAS, 313, 338
 Quirk W. J., 1972, APJ, 176, L9
 Rana N. 1991, ARA&A, 29, 129
 Rand R., Kulkarni S., Rice W., 1992, ApJ, 390, 66
 Regan M. W., Thornley M. D., Helfer T. T., Sheth K., Wong T., Vogel S. N., Blitz L., Bock D. C.-J., 2001, ApJ, 561, 218
 Romeo A. B., 1992, MNRAS, 256, 307
 Rots A., 1975, A&A, 45, 43
 Rownd B. K., Young J. S., 1999, AJ, 118, 670
 Rubin V. C., Waterman A. H., Kenney J. D. P., 1999, AJ, 118, 236
 Sage L., 1993, A&A, 272, 123
 Sanders D. B., Solomon P. M., Scoville N. Z., 1984, ApJ, 276, 182
 chaye J., 2002, submitted to the Astrophysical Journal, astro-ph/0205125
 Schmidt M., 1959, ApJ, 129, 243
 Silk J., 1997, ApJ, 481, 703
 Skillman E. D., Kennicutt R. C., Shields G. A., Zaritsky D., 1996, ApJ, 462, 147
 Sofue Y., Tutui Y., Honma M., Tomita A., Takamiya T., Koda J., Takeda Y., 1999, ApJ, 523, 136
 Sperandio M., Chincarini G., Rampazzo R., de Souza R., 1995, A&AS, 110, 279
 Toomre A., 1964, ApJ, 139, 1217
 Toomre A., 1981, Structure and Evolution of Normal Galaxies, 111
 van der Kruit P. C., 1974, ApJ, 192, 1
 van Zee L., Salzer J., Haynes M., O'Donoghue A., Balonek T., 1998, AJ, 116, 2805
 Vega Beltrán J. C., Pizzella A., Corsini E. M., Funes J. G., Zeilinger W. W., Beckman J. E., Bertola F., 2001, A&A, 374, 394
 Wang B. , Silk J., 1994, ApJ, 427, 759
 Warmels R., 1986, PhD thesis, Groningen Rijksuniversiteit
 Wevers B., van der Kruit P., Allen R., 1986, A&AS, 66, 505

Wong T. , Blitz L., 2002, ApJ, 569, 157
Wyse R. F. G., Silk J., 1989, ApJ, 339, 700
Young J. S. et al., 1995, ApJS, 98, 219
Zaritsky D., Kennicutt R., Huchra J., 1994, ApJ, 420, 87